Influence of the morphology on the translational and collective dynamics in ordered diblock copolymer melts

2005 J. Phys.: Condens. Matter 17 R551

(http://iopscience.iop.org/0953-8984/17/17/R01)

INSTITUTE OF PHYSICS PUBLISHING JOURNAL OF PHYSICS: CONDENSED MATTER

J. Phys.: Condens. Matter **17** (2005) R551–R570 doi:10.1088/0953-8984/17/17/R01

TOPICAL REVIEW

Influence of the morphology on the translational and collective dynamics in ordered diblock copolymer melts

C M Papadakis[1,3] **and F Rittig**[2]

[1] Physikdepartment E13, Technische Universität München, James-Franck-Straße 1, D-85747 München, Germany
[2] BASF AG, Polymer Research, GKP-G200, D-67056 Ludwigshafen, Germany

E-mail: Christine.Papadakis@ph.tum.de

Received 4 May 2004, in final form 15 March 2005
Published 15 April 2005
Online at stacks.iop.org/JPhysCM/17/R551

Abstract

Diblock copolymers in the melt state form a variety of mesoscopically ordered morphologies, depending on their composition and on temperature. They can thus serve as a model system for studying the dynamics in different ordered morphologies with the disordered state as a reference state. In this review, the methods for studying the dynamics are compiled. The dynamics in the disordered, the lamellar, the gyroid, the hexagonal and the body-centred cubic phase are described with particular emphasis on the polymer self-diffusion as well as on the collective dynamics. The dimensionality of the morphology has a strong influence on the dynamics: the copolymer diffusion along the interfaces is anisotropic, in contrast to the isotropic disordered phase, and collective motions such as undulations of lamellar interfaces or fluctuation of the micellar distance in the body-centred cubic state become possible.

Contents

[3] Author to whom any correspondence should be addressed.

1. Introduction

Diblock copolymers are linear polymers consisting of two chemically distinct blocks which usually repel each other. In the melt, they form a variety of ordered morphologies besides the disordered state, e.g. the lamellar, the gyroid, the hexagonal and the body-centred cubic structure. Both the morphology and the length scale of the structure formed can be controlled by the diblock copolymer architecture. The great variety of structures together with the possibility to tune both the length scale and the strength of the repulsive interaction between different blocks make diblock copolymer melts an ideal model system for studying the influence of the structure on the single-chain as well as on the collective dynamics.

A number of analogies between the dynamics of ordered block copolymer melts and other systems may be drawn. The lamellar state has many similarities with the smectic phase in liquid crystals. In both systems, the lamellar interfaces have been found to undulate (Ribotta *et al* 1974, Štěpánek *et al* 2001). Also, both in ordered block copolymer melts and in lyotropic lipid or surfactant systems, anisotropic diffusion has been observed (e.g. Nydén and Söderman 1995, Hillmyer *et al* 1996, Joabsson *et al* 1997, Feiweier *et al* 2000 and the results presented below). Investigations on solvated low molar mass components may suffer from the finite permeability of the surfactant layers to the water and from hydration effects. The block copolymer systems do not exhibit such effects: they are one-component systems, which reduces the degree of ambiguity. Another interesting aspect of block copolymer melts is the fact that diffusion proceeds in structures formed by self-organization, in contrast to host–guest systems such as nanoporous solids (Kärger *et al* 2004). Finally, block copolymer melts have the advantage that the length and timescales are more easily tunable than in other soft matter systems.

In this topical review, we focus on the relationship between the block copolymer morphology and the translational and collective dynamics. In the disordered state, the copolymers diffuse isotropically. In the lamellar and hexagonal state, on the other hand, the thermodynamic repulsion between the two blocks leads to predominantly two- or one-dimensional copolymer diffusion along the interfaces, respectively. In the gyroid state, chain diffusion along the interfaces takes place in three dimensions; however, it is retarded by the network structure. The cubic micellar state appears qualitatively different, because copolymer diffusion along the interfaces does not correspond to long-range diffusion. In all cases, entanglements may have an additional influence.

In the following, we will present results from our recent studies on several poly((ethylene propylene)-*b*-dimethylsiloxane) (PEP-PDMS) diblock copolymers using photon correlation spectroscopy and pulsed field gradient NMR, and compare them to the findings reported in the literature. With the PEP-PDMS system, we could study the slow collective dynamics as well as polymer self-diffusion in several morphologies while keeping the monomer pair the same and only varying the block lengths, i.e. the chemical details were not altered from sample to sample. In addition, temperature variation allows one to bring the system into the disordered, homogeneous state, which may serve as a reference state.

In reviewing results from the literature, we restrict ourselves to the translational and collective dynamics in diblock copolymer melts in thermodynamic equilibrium and in the absence of solvent. The reader is referred to the reviews by Mortensen (2000) on the structures in diblock copolymers under shear and under pressure, by Anastasiadis (2000) on the dynamics in diblock copolymers near the order-to-disorder transition (ODT) in the melt and in a common

good solvent, and by Fredrickson and Bates (1996), Colby (1996) and Baltá Calleja and Roslaniec (2000) on the dynamic mechanical properties of diblock copolymer melts. The present review is organized as follows. In section 2, the phase behaviour of the PEP-PDMS diblock copolymer system is briefly reviewed. In section 3, commonly used experimental methods for studying the slow dynamics in block copolymer melts are described. In section 4, recent progress is summarized. We conclude and present new perspectives in section 5.

2. The melt phase behaviour of diblock copolymers

Diblock copolymer melts form a variety of phases, depending on the volume fraction of one block, f, and the product χN of the Flory–Huggins segment–segment interaction parameter, χ, being inversely proportional to temperature, and the overall degree of polymerization, N; see the reviews by Folkes and Keller (1973), Bates and Fredrickson (1990), Bates (1991), Lodge (1994), Hasegawa and Hashimoto (1996), Hashimoto (1996), Ryan and Hamley (1997), Hamley (1998) and Baltá Calleja and Roslaniec (2000). Among the most prominent morphologies are the lamellar, the hexagonal and the body-centred cubic (bcc) phase. Also a bicontinuous phase (the gyroid phase), consisting of two continuous and isotropic networks of the minority component in a continuous matrix of the majority component, has been detected (Schulz *et al* 1994, Hajduk *et al* 1994). Two metastable structures, a hexagonally perforated and a hexagonally modulated lamellar structure, have been identified as well (Hamley *et al* 1993, 1994, Qi and Wang 1996, Laradji *et al* 1997). The ODT is a weak first-order phase transition (Fredrickson and Helfand 1987, Bates *et al* 1988) with concentration fluctuations in the disordered state close to the ODT. The repeat distance has been found to scale with the overall degree of polymerization, with the exponent being related to the degree of segregation: in the Gaussian regime ($\chi N < 5$), the chains are ideal; in the intermediate-segregation regime ($5 < \chi N < 30$) they start to stretch, and the domains start to demix; and in the strong-segregation limit ($\chi N > 30$) they are strongly stretched with narrow interfaces between the domains (Hashimoto *et al* 1980, Hadziioannou and Skoulios 1982, Richards and Thomason 1983, Matsushita *et al* 1990, Almdal *et al* 1990, Papadakis *et al* 1996, 1997).

A number of methods have been applied to investigate the phase behaviour of diblock copolymer melts, such as transmission electron microscopy (TEM), dynamic mechanical spectroscopy (DMS) and small-angle x-ray and neutron scattering (SAXS and SANS, respectively). Both SAXS and SANS have proven to be particularly useful for the determination of the repeat distances, and the unambiguous crystallographic identification of the ordered morphologies as well as the phase transitions (Lodge 1994, Hashimoto 1996, Ryan and Hamley 1997, Hamley 1998, Mortensen 2000). Most often, a certain number of higher-order reflections are necessary, and thus good scattering contrast between the blocks is desirable. For SANS, this can be achieved by selective deuteration of one of the blocks.

Shear alignment is a convenient way to obtain macroscopically oriented samples, which may help in identifying the ordered morphology. One example is given in figure 1: a compositionally asymmetric PEP-PDMS sample with a partially deuterated PEP block was mounted in the sandwich shear cell of a modified RSA II rheometer in the neutron beam (figure 1(a)). Macroscopic orientation of the sample was obtained by applying large-amplitude oscillatory shear. The scattered intensity monitored on a two-dimensional detector displays numerous reflections which can successfully be indexed by the twinned body-centred cubic morphology with the micelles on the lattice sites (figure 1(b), Papadakis *et al* 2004).

In this way, the phase diagram of a number of low molar mass PEP-PDMS diblock copolymers could be identified as a function of temperature and the volume fraction of PEP (figure 1(c), Vigild 1997, Papadakis *et al* 1999, 2004). For all values of f_{PEP}, the disordered

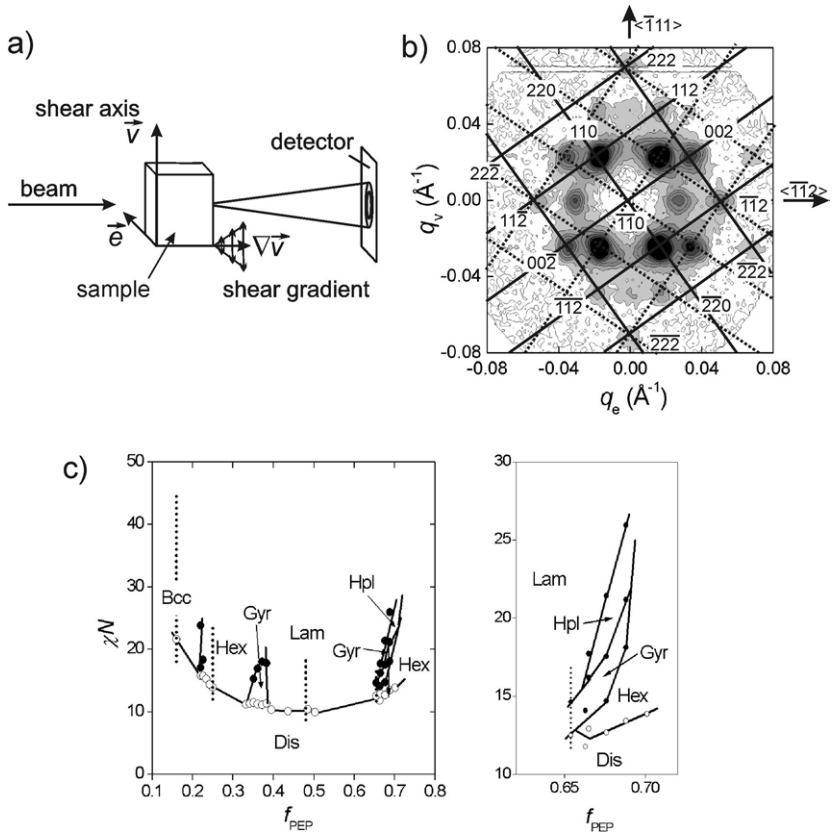

Figure 1. (a) The setup used for SANS on a shear-oriented sample. The shear direction ($\vec{v}$) is vertical and the shear gradient ($\nabla\vec{v}$) horizontal and parallel to the neutron beam. $\vec{e}$ denotes the neutral direction. The detector is an area detector. The use of this setup was first described by Vigild *et al* (1998). (b) Two-dimensional SANS spectrum from a PEP-PDMS sample (molar mass 23 600 g mol^{-1}, volume fraction of PEP 0.16) measured at 24 °C after shear alignment and equilibration at the same temperature. The intensity scale is logarithmic and ranges from white (low intensity) to black (high intensity), covering three decades. The full and dotted lines indicate the reciprocal lattice expected for a twinned bcc structure with the common $\langle\bar{1}11\rangle$-axis parallel to $\vec{v}$ and the $\langle\bar{1}\bar{1}2\rangle$-axis parallel to $\vec{e}$. The indexing is given for the domain marked by full lines. From Papadakis *et al* (2004). (c) Resulting phase diagram of PEP-PDMS. (○) and (●): ODTs and order–order transitions, OOTs (Vigild 1997, Papadakis *et al* 1999, 2004). The black lines indicate the resulting approximate locations of the phase boundaries. Bcc, Hex, Gyr, Lam and Dis stand for the body-centred cubic, the hexagonal, the gyroid, the lamellar and the disordered phase, and Hpl denotes the metastable hexagonally perforated layer structure. The vertical dotted lines mark the samples presented in the present publication and the χN-ranges studied. The right panel shows the high-f_{PEP} region.

state is encountered at low χN. Between 0.38 and 0.65, the system orders into the lamellar state; with increasing compositional asymmetry, the gyroid, the hexagonal and the bcc states are encountered. The hexagonally perforated layer morphology was found to be metastable with respect to the gyroid phase (Vigild *et al* 1998).

We have studied the translational dynamics of four symmetric and asymmetric PEP-PDMS diblock copolymers in the melt, which form the lamellar, the gyroid, the hexagonal and the body-centred cubic state below the ODT temperature and the disordered state above. Before

presenting the results, we wish to review some of the experimental methods used for such investigations.

3. Experimental methods for studying the dynamics

A number of experimental methods have been used for studying the structure and dynamics of mesoscopically structured diblock copolymer systems. The most commonly used experimental techniques include forced Rayleigh scattering (FRS), forward recoil spectroscopy (FRES), nuclear reaction analysis (NRA), secondary ion mass spectroscopy (SIMS), photon correlation spectroscopy (PCS) and pulsed field gradient (PFG) NMR.

FRS has been used to measure the self-diffusion coefficients of fluorescent tracers through diblock copolymer melts in a large range of diffusivities (10^{-9}–10^{-21} m^2 s^{-1}), Ehlich *et al* 1993, Dalvi and Lodge 1993, 1994, Lodge and Dalvi 1995, Zielinski *et al* 1995, Hamersky *et al* 1996, Lodge and Chapman 1997, Lodge *et al* 1997, Hamersky *et al* 1998a, 1998b, Cavicchi and Lodge 2003, 2004. Usually, fluorescent groups are chemically attached to a small amount (approximately 5%) of the diblock copolymers. By means of two interfering laser beams incident on the sample under a certain angle, the fluorescent tracers are bleached by the laser light, and a hologram is created in the sample. The grating distance, d, and thus the length scale probed are determined by the angle between the two laser beams and by their wavelengths. After turning off one of the laser beams, the decay of the grating due to diffusion of the fluorescent polymers is read out by monitoring the decay of one of the diffraction peaks of the second beam. In the case of isotropic diffusion, the decay is expected to be exponential with a decay time τ. The diffusion coefficient is calculated from $D = d^2/(4\pi^2\tau)$.

In FRES, a beam of helium ions hits the sample surface, and from the energy spectrum of recoiled protons and deuterons, their depth-dependent distribution within the film is determined with a spatial resolution of the order of 80 nm (Doyle and Peercy 1979, Mills *et al* 1984). The method has been applied for measuring the changes of the concentration profile of deuterium in a specially prepared layer structure (Shull *et al* 1991, Yokoyama and Kramer 1998, 2000a): a layer of deuterated diblock copolymers is placed on a layer of non-deuterated diblock copolymers. The changes in concentration profile near the layer interface are related to the polymer self-diffusion coefficient.

SIMS offers a better spatial resolution ($\sim$15 nm, Yokoyama *et al* 1998, Yokoyama and Kramer 2000b) and allows one to monitor the concentration profiles of groups present in one of the blocks only. For this purpose, primary ions of lower energy than in FRES are used, and secondary ions are detected while eroding the polymer sample. The variation of the concentration profile with time is related to the polymer self-diffusion coefficient.

NRA is another method to measure the concentration profile of deuterated tracers and to determine the polymer diffusion coefficient by monitoring its temporal changes (Chaturvedi *et al* 1990, Budkowski *et al* 1995). The setup is similar to FRES in that a thin layer of deuterated material made by spin coating is placed on top of or between the regular matrix. After annealing, the composition depth profiles of the deuterated segments normal to the polymer films are determined using non-resonant NRA, based on the reaction $^3\mathrm{He} + {}^2\mathrm{H} \rightarrow {}^4\mathrm{He} + {}^1\mathrm{H} + \text{energy}$. An He beam impinges on the polymer film and penetrates the sample, whereby it loses its energy. From the energy spectrum of the ^{4}He species scattered at forward angle and the calibrated energy losses of the incident and scattered particles, the composition depth profile of the deuterium is determined. The diffusion coefficient is deduced from the changes of the profile of the interface of a bilayer with one of the layers containing deuterated polymer. In the NRA experiment, a spatial resolution of 3 nm may be reached (Kerle *et al* 1997).

PCS allows one to study the collective dynamics in a large time range (microseconds to seconds). The fluctuations of the intensity of the scattered laser light are recorded as a

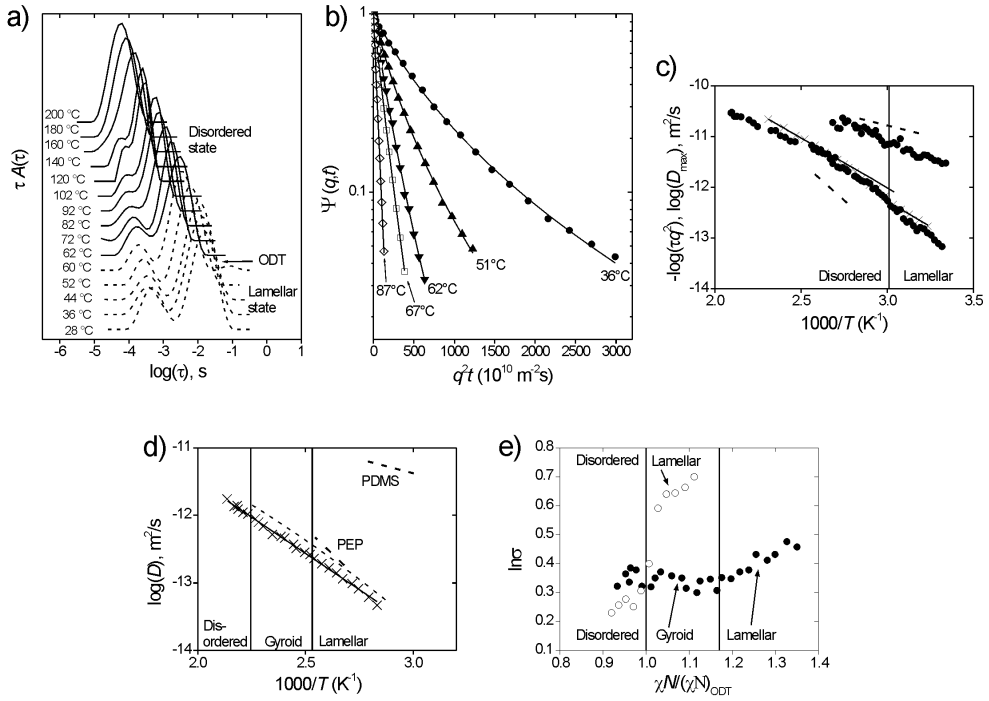

Figure 2. Results from the PEP-PDMS diblock copolymer samples forming the lamellar and gyroid morphology: (a)–(c) $\bar{M}_n = 6300$ g mol^{-1} and $f_{\mathrm{PEP}} = 0.48$. (a) Distribution functions of relaxation times from PCS, (b) echo attenuation curves from PFG NMR at different temperatures together with fits of equation (8), (c) $(q^2\tau)^{-1}$-values from PCS (●) and average self-diffusion coefficients from PFG NMR ($D_{\max}$, ×) in an Arrhenius representation. The lines are linear fits to the PFG NMR data. From Štěpánek *et al* (1997) and Fleischer *et al* (1999). (d) Self-diffusion coefficients $D_{\max}$ from PFG NMR (×) on a PEP-PDMS sample with $\bar{M}_n = 10\,600$ g mol^{-1} and $f_{\mathrm{PEP}} = 0.65$. The full line is a fit to the data, and the dashed line indicates the diffusion coefficients in the hypothetical homogeneous state. From Rittig *et al* (2001). In (c) and (d), the thick dashed lines indicate the self-diffusion coefficients of the homopolymers having the same molar mass as the diblock copolymers (Shull *et al* 1991, Appel and Fleischer 1993, Pearson *et al* 1994). (e) Widths of the distributions of self-diffusion coefficients from PFG NMR. From Fleischer *et al* (1999) and Rittig *et al* (2001). In (c)–(e), the vertical lines denote the ODTs and the OOT.

function of time with a resolution of less than 100 ns. Experiments are conducted as a function of scattering angle. The autocorrelation function of the scattered intensity, $g_2(t)$, is calculated online and allows one to determine the characteristic relaxation times, τ. This is often carried out by an inverse Laplace transformation (ILT) of $g_2(t)$:

$$g_2(t) - 1 = f^* \left(\int A(\tau) \exp(-t/\tau)\, \mathrm{d}\tau \right)^2, \tag{1}$$

where f^* is the coherence factor and $A(\tau)$ the distribution function of relaxation times. The programs CONTIN (Provencher 1982) or REPES (Jakeš 1988), for instance (a comparison of these and other routines has been given by Štěpánek (1993)), perform the ILT numerically, and the characteristic relaxation times are extracted as the centres of mass of the peaks in $A(\tau)$ (see, for instance, figure 2). Subtraction of single decays (i.e. peaks in the distribution function of relaxation times) from the correlation curve has in some cases proven useful before re-analysing the remaining curve using REPES (Štěpánek and Johnsen 1995, Papadakis *et al*

1996, Štěpánek and Lodge 1996b). The subtraction was not found to influence the relaxation rates and amplitudes of the remaining modes.

PFG NMR is a method to study the long-range polymer self-diffusion. The length scales monitored range from ∼500 Å to several micrometres with observation times t between 13 and 603 ms. The fundamentals and applications have been described by Kärger *et al*, (1988, 1998) and by Callaghan (1993). The NMR signal may be generated by the stimulated echo rf-pulse sequence. Applying field gradient pulses after the first and third $\pi/2$-rf-pulse, respectively, leads to an attenuation of the echo due to polymer diffusion along z. For homogeneous systems, the choice of a Gaussian propagator is appropriate for displacements exceeding the polymer radius of gyration. Then, the echo attenuation is given by

$$\Psi(q,t) = \int \exp(\mathrm{i}qz)\exp(-q^2tD)\,\mathrm{d}z. \tag{2}$$

The magnitude of the generalized scattering vector $q = \gamma\delta g$ is the product of the gyromagnetic ratio γ of the proton and the width (δ) and amplitude (g) of the gradient pulses, respectively (Fleischer and Fujara 1994). D is the self-diffusion coefficient related to the mean-square displacement $\langle z^2\rangle$ of the polymer segments in the gradient direction during the observation (or diffusion) time t by the Einstein equation:

$$\langle z^2\rangle = 2Dt. \tag{3}$$

If the echo attenuation curves $\Psi(q,t)$ versus q^2t measured with different observation times t merge into master curves, the diffusion is unrestricted over the considered observation times and length scales. It has very recently become possible to identify the species in multicomponent samples giving rise to the PFG NMR signal (Kärger *et al* 2003, 2004).

There is a substantial difference between the principles of detection of PCS and PFG NMR. The intensity fluctuations detected in PCS as a function of time are due to fluctuations of the refractive index of the sample, which, in diblock copolymer melts, mainly have fluctuations of the monomer concentrations at their origin. The physical processes at the origin of the fluctuations observed need to be deduced from the q- and temperature-dependence of the relaxation rate. PFG NMR, on the other hand, monitors the molecular displacements, i.e. the long-range self-diffusion. In both types of experiments, the monitored length scales of motion are larger than the repeat distances of the lattices formed by the PEP-PDMS samples described here. By comparison of the values of $(q^2t)^{-1}$ obtained from PCS with the PFG NMR long-range self-diffusion coefficients, more information about the underlying mechanisms can be gained.

4. Collective dynamics and self-diffusion of diblock copolymers in different melt morphologies

In this section, we describe results on the slow dynamics in different morphologies, both from the literature and from our studies on several PEP-PDMS diblock copolymer melts, in the lamellar, the gyroid, the hexagonal and the body-centred cubic morphology and the disordered phase. A number of factors have an additional influence on the dynamics, such as the morphology, the strength of the repulsive interaction between the two blocks, described by the χ-parameter, and the degree of entanglement. Experimental studies are limited, though, by the glass transition temperatures of the two blocks (setting a lower limit to the temperature range where diffusion, for instance, can take place) as well as degradation of the polymer (setting an upper limit to the accessible temperature range).

The PEP-PDMS system proves to be an ideal system for studies of the slow dynamics in different morphologies. The low glass transition temperatures (−56 °C) and high degradation

Table 1. Characteristics of the PEP-PDMS samples studied by us. $\bar{M}_n$: number average of the overall block copolymer molar mass, N: degree of polymerization based on a segment volume of 118 Å^3, f_{PEP}: volume fraction of the PEP block from stoichiometry and NMR, T_{ODT} and T_{OOT}: ODT and OOT temperatures. $\bar{M}_w/\bar{M}_n = 1.1$ for all samples (Vigild 1997). The PEP blocks are partially deuterated. The χ-parameter of the PEP/PDMS pair is 41.4 K$/T - 0.024$ (Almdal *et al* 2002). The entanglement molar masses of PEP and PDMS are 1500 and 13 000 g mol^{-1}, respectively (Fetters *et al* 1994). The glass transition temperatures of PEP and PDMS are −56 °C (Bates *et al* 1989) and −127 °C (Brandrup and Immergut 1989).

Morphology in ordered state	$\bar{M}_n$ (g mol^{-1})	N	f_{PEP}	T_{ODT} (°C)	T_{OOT} (°C)	Repeat distance (Å)
Lamellar	6300	105	0.48	64	—	100–110
Gyroid and lamellar	10 600	181	0.65	172	122	145–165[a]
Hexagonal	13 000	211	0.25	187	—	250–270
Body-centred cubic	23 600	381	0.16	273	—	220–250

[a] $2\pi/q^*$, where q^* is the position of the first-order Bragg reflection (Almdal *et al* 1996).

temperatures (∼300 °C) make a large temperature range accessible, allowing systematic studies of the temperature dependence of the processes identified. In addition, because of its relatively high χ-parameter, the ODT temperatures are accessible already for low molar mass, i.e. some of the samples are non-entangled even in the ordered morphologies. The characteristics of the PEP-PDMS samples studied by us are compiled in table 1.

4.1. The disordered state

In the disordered state, an analytical mean-field treatment is possible, and two dynamic processes have been predicted:

- the internal mode, due to the relative translational motion of the two blocks (Akcasu and Tombakoglu 1990, Borsali and Vilgis 1990, Genz and Vilgis 1994), and
- the diblock copolymer self-diffusion (Semenov *et al* 1994, Fytas *et al* 1994).

In a later approach, microscopic polymer-mode-coupling theory has been used to treat the influence of fluctuations near the ODT, the formation of an ordered mesophase and entanglements on the block copolymer self-diffusion (averaged over all spatial directions, Tang and Schweizer 1995, Guenza *et al* 1997, 1998, Guenza and Schweizer 1998). The translational motion was found to be retarded near and below the ODT in a thermally activated manner. The suppression of the diffusion increases with diblock copolymer molar mass, for instance. A wealth of experimental studies have addressed the dynamics in the disordered state; see the reviews by Fytas and Anastasiadis (1994), Colby (1996), Fredrickson and Bates (1996), Štěpánek and Lodge (1996a, 1997) and Anastasiadis (2000) as well as the report on several chemically different samples by Štěpánek and Lodge (1996b). Both the internal mode (Anastasiadis *et al* 1993a, Vogt *et al* 1994, Štěpánek and Lodge 1996b) and the copolymer self-diffusion were observed in numerous experiments with PCS (Shull *et al* 1991, Anastasiadis *et al* 1993a, 1993b, Vogt *et al* 1993, 1994, Fleischer *et al* 1993, 1997, 1999, Dalvi and Lodge 1994, Fytas *et al* 1994, Papadakis *et al* 1996, Štěpánek and Lodge 1996b, Lodge *et al* 1997, Štěpánek *et al* 1997).

In addition to these predicted processes, the segmental dynamics (Gerharz *et al* 1991, Kanetakis and Fytas 1991, Kanetakis *et al* 1992, Vogt *et al* 1992, Hoffmann *et al* 1993) were detected using PCS. Another mode which came unexpectedly was observed to have a q-independent relaxation time and to give rise to depolarized scattering. It was tentatively

assigned to the reorientation of the stretched chains or of transient microphase-separated domains close to the ODT (Hoffmann *et al* 1993, Jian *et al* 1994, Papadakis *et al* 1996) or to the rotational diffusion of the clusters mentioned below (Štěpánek *et al* 1997). In addition, a slow mode with a relaxation rate proportional to q^2 was detected as well and—its origin being unclear—was termed 'cluster mode' (Anastasiadis *et al* 1993a, Papadakis *et al* 1996, 2000a, 2000b, Štěpánek and Lodge 1996b, 1997). In the following, we are going to describe the characteristics of all five modes in more detail.

The segmental dynamics of the two types of segments in a diblock copolymer give rise to two decays in the depolarized PCS curve (i.e. measured with the sample between crossed polarizers), each being broad and having a strong temperature dependence, as the glass transition temperature of the respective block is approached. In some cases, the timescales of the segmental dynamics of the two blocks overlap, and the decays can therefore not be separated, leading to a single, broad decay (Kanetakis and Fytas 1991).

The internal mode is related to the internal chain dynamics, i.e. to the longest Rouse mode, which corresponds to a relative movement of the two blocks. It has a relaxation rate which is independent of the scattering vector q, provided the molar mass is not too high (Akcasu and Tombakoglu 1990, Borsali and Vilgis 1990). Its light scattering amplitude increases with NR_g^2 (Fytas *et al* 1994), where N is the overall degree of polymerization and R_g the polymer radius of gyration, i.e. it gives rise to significant scattering only for high molar masses. For the PEP-PDMS samples studied by us (table 1), it was estimated to have a relaxation time of the order of microseconds, and was thus outside the experimentally accessible time range of PCS (Štěpánek *et al* 1997). A series of PCS studies has addressed the dynamic structure factor deep in the disordered state as well as close to the ODT using a series of ultrahigh molar mass diblock copolymers in non-selective, good solvent (Sigel *et al* 1999, Holmqvist *et al* 2002, 2003). With this kind of sample, the length scale of composition fluctuations is so large that the peak of the structure factor is in the q-range of light scattering. By comparing the dynamic and static parts of the dynamic structure factor, $S(q, t)$, these authors could show that, for monodisperse block copolymers, the internal mode is at the origin of the peak in the static structure factor, $S(q)$, and that its relaxation rate decreases slightly in the vicinity of the peak position due to the repulsion between the two blocks.

Using depolarized PCS, an additional mode with a q-independent relaxation rate was observed in poly(styrene-*b*-isoprene) (Hoffmann *et al* 1993), poly(styrene-*b*-methylphenylsiloxane) (Jian *et al* 1994), poly(styrene-*b*-butadiene) (Papadakis *et al* 1996) and PEP-PDMS (Štěpánek *et al* 1997). Close to the ODT, its amplitude is significant. It was tentatively attributed to the stretching and the reorientation of the copolymer blocks due to the concentration fluctuations; however, the reorientation of local lamellar regions, which possibly are related to the clusters, may also be at the origin of this mode (Štěpánek *et al* 1997).

The heterogeneity mode observed in PCS has been identified to be due to block copolymer self-diffusion. This has been shown by comparing the diffusion coefficient deduced from the q^2-dependent PCS relaxation rate with the self-diffusion coefficient obtained by PFG NMR (Fleischer *et al* 1999 and figure 2(c)). The relation between D_{het} and D_{self} has for symmetric samples in the disordered state been predicted to read (Semenov *et al* 1994)

$$D_{het} = D_{self}[1 - 2\chi N(\delta f)^2] \qquad \text{with } (\delta f)^2 = \frac{\bar{M}_w - \bar{M}_n}{4\bar{M}_w}. \tag{4}$$

For the symmetric PEP-PDMS sample, equation (4) predicts a ratio $D_{het}/D_{self} \approx 0.5$–$0.6$, which is within the uncertainty of our PCS and PFG NMR measurements. The heterogeneity mode is observed in all PEP-PDMS samples studied by us (figures 2(a), 3(b) and 4(a)–(c)) and shows the usual characteristics.

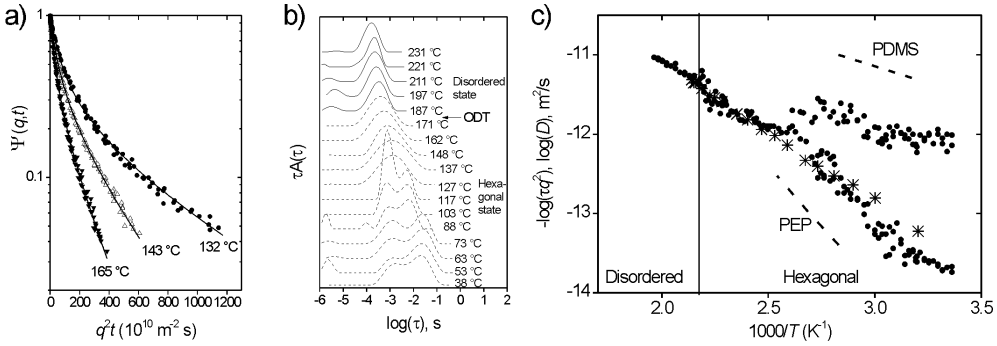

Figure 3. Results from the PEP-PDMS diblock copolymer sample forming the hexagonal morphology: $\bar{M}_n = 13\,000$ g mol^{-1} and $f_{PEP} = 0.25$. (a) PFG NMR echo attenuation curves and (b) PCS distribution functions at different temperatures. The full lines in (a) are fits of equation (10). (c) Arrhenius diagram, $(q^2\tau)^{-1}$-values from PCS (●) and average self-diffusion coefficients from PFG NMR (D_0, ∗). From Papadakis *et al* (2000b). The thick dashed lines indicate the self-diffusion coefficients of the homopolymers having the same molar mass as the diblock copolymers. The vertical line denotes the ODT.

Furthermore, a slow, diffusive mode has frequently been observed in diblock copolymer melts and was termed the cluster mode (Anastasiadis *et al* 1993b, Papadakis *et al* 1996, 2000a, 2000b, Štěpánek and Lodge 1996b, Štěpánek *et al* 1997). Its origin is unclear, but it has been speculated that it is related to the onset of microphase separation near the ODT (Chitanvis 1998). The PEP-PDMS system is ideal to test this hypothesis, as, due to the high degradation temperature, measurements can be extended to temperatures far above the ODT temperature. Contrary to expectation, the cluster mode was observed up to 300 °C with a significant temperature-independent amplitude in the correlation functions (40–90%, increasing with f_{PEP}). This is in contrast to the anticipated coupling to concentration fluctuations cited above. As reported for chemically different samples, the diffusion coefficients are very low (10^{-15}–10^{-13} m^2 s^{-1}) and correspond to hydrodynamic radii of the diffusing entities being much larger (e.g. ∼1300 Å for a sample with $\bar{M}_n = 12\,500$ g mol^{-1} and $f_{PEP} = 0.22$ between the ODT temperature of 134 and 250 °C) than the polymer radii of gyration ($\lesssim$200 Å). We conclude that not all factors at the origin of the cluster mode have been identified yet.

4.2. The lamellar morphology

The lamellar structure formed by symmetric diblock copolymers may be considered as a periodic potential having a severe impact on the copolymer diffusion because of the repulsive interaction between different blocks. It was predicted by Barrat and Fredrickson (1991) that the diffusion of symmetric diblock copolymers with Rouse dynamics through a periodic potential is slowed down significantly. A possible mechanism of diffusion was suggested by Helfand (1992): in the strong-segregation limit, diffusion of the copolymer across the lamellar interfaces proceeds via strong stretching of one block through the chemically different part of the lamellae. In this way, the number of contacts between different segments is minimized. Molecular-dynamics simulation of the diffusion of diblock copolymers based on the Rouse model confirmed that their diffusion *across* the lamellar interfaces is strongly slowed down as the repulsion between the segments, χ, is increased, whereas the diffusion coefficient *parallel* to the interfaces is nearly independent of χ (Murat *et al* 1998).

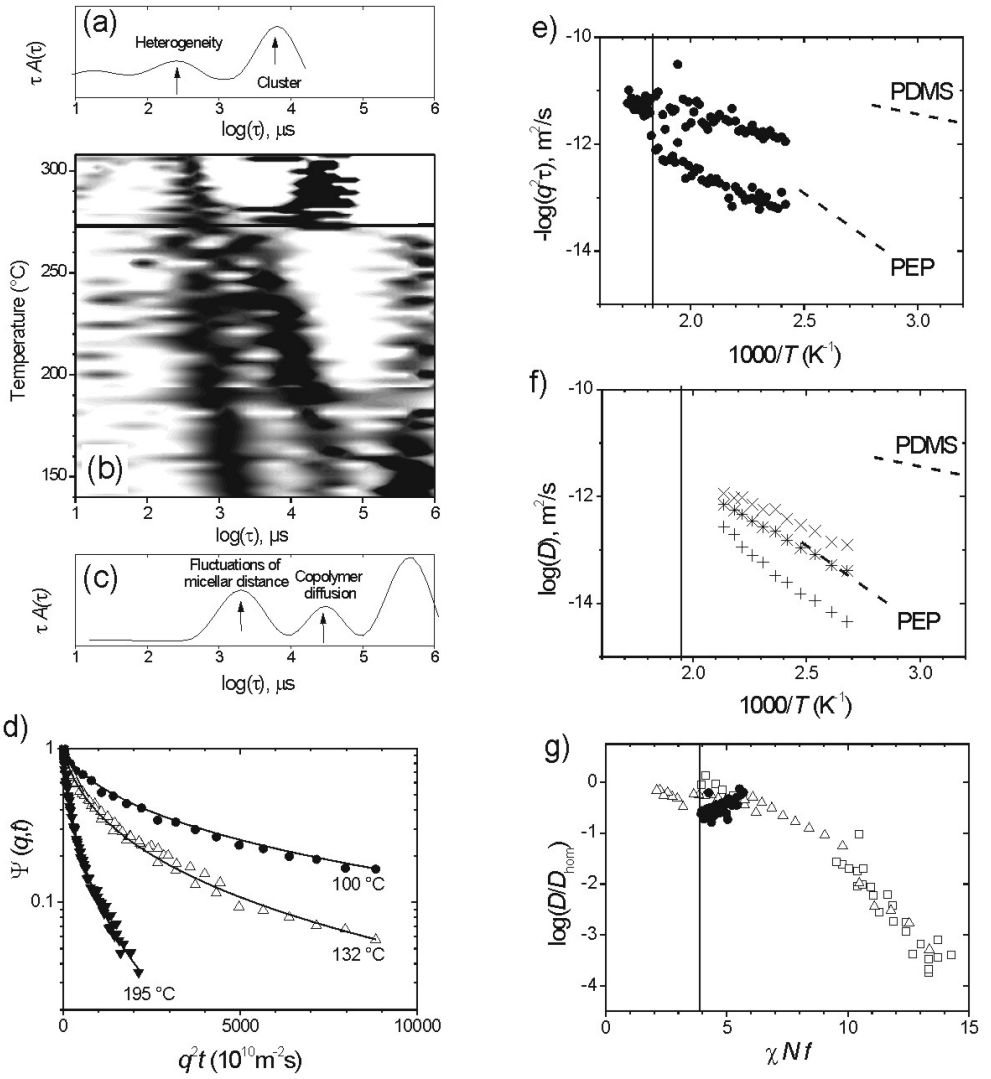

Figure 4. Results from the PEP-PDMS diblock copolymer sample forming the body-centred cubic morphology: $\bar{M}_n = 23\,600$ g mol^{-1} and $f_{\mathrm{PEP}} = 0.16$. (a)–(c) PCS distribution functions. In (b), the amplitude scale is linear and ranges from zero (white) to one (black). The horizontal black line indicates the ODT. (d) PFG NMR echo attenuation curves. The full lines are fits of equation (8). (e) $(q^2\tau)^{-1}$-values from PCS (●). The thick dashed lines indicate the self-diffusion coefficients of the homopolymers having the same molar mass as the diblock copolymers. The vertical line denotes the ODT. (f) Average self-diffusion coefficients from PFG NMR (×: $D_{\max}$, ∗: D_0, +: $\bar{D}$). (g) Semi-logarithmic representation of D/D_{hom} of the slow PCS mode versus $\chi N f_{\mathrm{PEP}}$ (●). The vertical line denotes the ODT of our PEP-PDMS sample. Data from the literature: (△) asymmetric PEP-PDMS diblock copolymers with PDMS being the minority component (Cavicchi and Lodge 2003), (□) asymmetric PS-P2VP diblock copolymers with P2VP being the minority component (Yokoyama and Kramer 1998). (a)–(c), (g) from Papadakis *et al* (2004).

Indeed, in a number of experiments, non-entangled diblock copolymers have been found to diffuse mainly along the lamellar interfaces, i.e. in two dimensions. In FRS and PFG NMR experiments on PEP-PEE diblock copolymers, the anisotropy of diffusion (i.e. the ratio of the diffusion coefficients parallel and perpendicular to the lamellar interface, $D_{\mathrm{par}}/D_{\mathrm{perp}}$) could

be quantified (Dalvi and Lodge 1993, Hamersky *et al* 1998b, Fleischer *et al* 1999, Rittig *et al* 2001). For well-entangled diblock copolymers, however, the anisotropy of diffusion was found to be small, and the copolymer diffusion parallel to the interface was suggested to proceed via a block retraction mechanism (Lodge and Dalvi 1995). In all cases, the diffusion perpendicular to the interface is an activated process, because the blocks have to overcome the barrier made up by the lamella formed by the other block. The diffusion coefficient perpendicular to the lamellar interfaces, D_{perp}, has repeatedly been found to follow the dependence

$$D_{\mathrm{perp}} = D_{\mathrm{hom}} \exp(-\alpha f \chi N) \tag{5}$$

with D_{hom} the diffusivity in the disordered, homogeneous state and α the activation barrier. The product αf was found to be 0.273 in macroscopically oriented poly(ethylene propylene-*b*-ethylethylene) diblock copolymer samples (Lodge and Dalvi 1995). For well-entangled, ultrahigh molar mass diblock copolymers in a common good solvent, Holmqvist *et al* (2003) identified $\alpha f = 0.05$–0.4 in the vicinity of the ODT for copolymers containing styrene and isoprene or ethylene-*alt*-propylene as comonomers. These samples had different compositions and concentrations in a common good solvent. The observed molar-mass dependence, $\alpha f \propto M$, was attributed to the role of entanglements having an influence on the apparent activation barrier.

In samples with the lamellar domains being isotropically oriented, D_{par} and D_{perp}, the anisotropy of diffusion has to be extracted from the average over all spatial dimensions,

$$D_{\mathrm{lam}} = \frac{2D_{\mathrm{par}} + D_{\mathrm{perp}}}{3}. \tag{6}$$

We have combined PCS and PFG NMR in order to study a non-aligned, low molar mass PEP-PDMS sample in a large temperature range around the ODT (figures 2(a), (b)). The echo attenuation curves from PFG NMR deviate from single-exponential shape (isotropic solution of equation (2)), which is due to a superposition of diffusivities along and across the lamellar interfaces with a certain anisotropy of diffusion (figure 2(b)). In principle, information on the anisotropy of diffusion can be extracted from an analysis of the shape of the PFG NMR echo attenuation curves. The resulting anisotropies, however, were low (<10, Rittig *et al* 2001). As defects of the lamellar structure may contribute significantly to the diffusivities and hamper a quantitative analysis, the description of the curves by a logarithmic distribution of the diffusion coefficients seemed more appropriate and fitted the curves well (figure 2(b), Fleischer *et al* 1999, Rittig *et al* 2001):

$$w(\ln D) \propto \exp\left[-\frac{\ln^2(D/D_0)}{2\ln^2\sigma}\right] \tag{7}$$

with D_0 the median value of the diffusivity and $\ln(\sigma)$ the width of the distribution. The echo attenuation curve then reads

$$\Psi(q,t) = \int w(\ln D) \exp(-q^2 t D) \mathrm{d}(\ln D). \tag{8}$$

The Arrhenius representation of the most probable diffusion coefficient, $D_{\mathrm{max}} = D_0 \exp(-\ln^2\sigma)$ (figure 2 c), reveals linear dependences both in the disordered and the lamellar state. Extrapolating these lines from the disordered and the lamellar state, a discontinuity of the diffusion coefficient at the ODT by a factor very close to $2/3$ is observed, i.e. the factor by which the diffusion is expected to be reduced at a transition from three- to two-dimensional diffusion (Callaghan 1993). Also the discontinuous increase of the width of the distribution, $\ln\sigma$, when entering the lamellar state (figure 2(e)) is indicative of this transition, since the lamellae are not macroscopically aligned (Fleischer *et al* 1999). Over the entire temperature

range studied, the slower one of the two modes observed in the PCS experiment on the same sample coincides with the average self-diffusion coefficients from PFG NMR (Štěpánek *et al* 1997, figures 2(a), (c)), indicating that this mode is due to spatially averaged copolymer self-diffusion through the lamellar structure (Fleischer *et al* 1999). This analysis of the shape of the echo attenuation curve thus gives insight into the influence of the structural changes on the self-diffusion. They can be observed in the PFG NMR experiment, but not in FRS experiments, because the diffusion distances measured are much shorter than in FRS, leading to incomplete averaging.

The faster process observed using PCS (figure 2(a)) has a relaxation rate proportional to q^2. The process could be assigned by means of a depolarized PCS experiment on the same sample, which was carefully oriented macroscopically. By rotating the sample in the laser beam, the angle between the scattering vector and the normal to the lamellar planes was varied. From the dependence of the relaxation rate on this angle, the fast process could be identified to be due to undulations of the lamellar interfaces (Štěpánek and Lodge 1996b, Štěpánek *et al* 2001). In analogy to smectic systems, the ratio between Γ and q^2 was found to be related to the splay elastic modulus K (Štěpánek *et al* 2001). K vanishes near the ODT temperature, where the translational long-range order is lost.

A mode having the same characteristics as the internal mode could be detected in the lamellar state of poly((ethylene propylene)-*b*-ethylethylene) using PCS (Štěpánek and Lodge 1996b). However, its temperature behaviour does not follow the Williams–Landel–Ferry equation (which is the case in the disordered state), and it was speculated that this mode observed in the lamellar state is due rather to composition fluctuations on a local scale than to the internal mode. In the PEP-PDMS samples studied by us, it is in the microseconds time-regime, and thus outside our experimental time window.

The behaviour of the cluster mode in the ordered state seems to depend on the nature of the sample: in poly(ethylene-*b*-ethylethylene), poly(ethylene-*b*-vinylcyclohexane) and in the PEP-PDMS diblock copolymer melts presented here, an abrupt and significant slowing-down is observed, when crossing the ODT into the lamellar state; in contrast, in poly((ethylene propylene)-*b*-ethylethylene) and poly(ethylethylene-*b*-vinylcyclohexane), no abrupt slowing down was observed (Štěpánek and Lodge 1996b). It is thus not straightforward to classify the behaviour of the cluster mode in the ordered state and in this way gain more information on its origin.

We conclude that the lamellar morphology has a severe impact on the block copolymer self-diffusion: it becomes anisotropic. In the (non-entangled) PEP-PDMS system, the analysis of the shape of the echo attenuation curve from PFG NMR allowed us to observe the effect of the lamellar structure even with a non-oriented sample. An additional mode observed in DLS experiments could in depolarized experiments on a macroscopically aligned sample be identified as being due to undulations of the lamellar interfaces. The behaviour of the cluster mode varies from system to system, the reason still being unclear.

4.3. The gyroid morphology

The dynamics in the gyroid structure is by far less investigated than the lamellar structure. One reason might be that the synthesis of polymers exhibiting this morphology is not trivial. The morphology consists of an arrangement of short rods (struts) in a matrix. Locally, one may expect an anisotropy of motion similar to the cylindrical case (see below). However, the length of the struts is much shorter than the shortest displacement observable by FRS or PFG NMR, for instance.

In an FRS study on a poly((ethylene oxide)-*b*-ethylethylene) (PEO-PEE) diblock copolymer sample forming the hexagonal cylindrical and the gyroid morphology as a function of temperature, an anisotropy of self-diffusion of ∼80 was found in the cylindrical phase (Hamersky *et al* 1998a). The FRS decays from the gyroid phase were single-exponential and gave a diffusivity consistent with the one parallel to the cylinder axis reduced by the tortuosity of the gyroid network. However, the copolymer diffusivity was lower than that of either of the constituent homopolymers or of other disordered PEO-PEE diblock copolymers, even after accounting for differences in molar mass. This was attributed to the onset of entanglement effects.

The gyroid structure in the PEP-PDMS diblock copolymer melt studied by us (Rittig *et al* 2001) consists of two interpenetrating PDMS networks in a PEP matrix (Almdal *et al* 1996). The self-diffusion coefficients from PFG NMR follow an Arrhenius law over the whole temperature range (figure 2(d)). No discontinuity is observed, either at the ODT between the gyroid and the disordered state or at the OOT between the gyroid and the lamellar state. In all three phases, the self-diffusion coefficients are lower than those of the slowest constituent homopolymer having the same molar mass as the diblock copolymer. This is surprising, because one would expect the diffusion coefficient of the diblock copolymer to be given by the average friction coefficient of the two blocks, thus lying between those of the homopolymers. One might argue that these low diblock copolymer diffusivities are a result of the influence of the morphology, having in mind that the copolymer diffusion path follows the interfaces of these structures. In order to estimate this effect, we have calculated a diffusion coefficient for a hypothetical, disordered diblock copolymer melt at the same temperature (Rittig *et al* 2001) by eliminating the effect of the higher path length for a chain diffusing along the interface, analogously to Anderson and Wennerström (1990). These authors computed the so-called obstruction factor (i.e. the reduction of the diffusivity compared to the disordered phase) for several systems, among them the bicontinuous cubic phase. For particle diffusion on a minimal surface exhibiting cubic symmetry (the gyroid morphology), the diffusivity is reduced by a factor of 1.5. The diffusion coefficient for the hypothetical disordered state at the same temperature is thus given by $D_{\mathrm{hy}} = 1.5 D_{\mathrm{max}}$, with D_{max} denoting the measured most probable self-diffusion coefficient in the gyroid morphology. However, even D_{hy} is lower than the slowest homopolymer (PEP, figure 2(d)).

One therefore needs to consider that the PEP block is entangled. While the pure homopolymer in an entangled melt would follow its tube, this is not possible for a diblock copolymer in the ordered state because the tube is perpendicular to the interface. This additional reduction has been described as an activated reptation and, for high χN-values, as a block retraction mechanism (Fredrickson and Milner 1990, Dalvi and Lodge 1993, Dalvi *et al* 1993). For the activated reptation across the interface, the chain has to overcome an enthalpic barrier which determines the diffusivity (equation (5)). In the case of a block retraction mechanism, the enthalpic barrier is so high that the diffusivity depends only on the number of entanglements per chain, and the self-diffusion coefficient is given by $D \propto \exp(-N/N_{\mathrm{e}})$, where N_{e} is the number of monomers between two entanglements (Dalvi *et al* 1993, Lodge and Dalvi 1995).

The combination of the copolymer diffusion along the interfaces of the gyroid structure with the influence of the entanglements thus leads to a drastic reduction of the self-diffusion coefficient with respect to the homogeneous disordered phase. Since the PDMS block is not entangled and the χN-values are relatively high, the diffusion in the PEP-PDMS system can probably be described by a block retraction mechanism where the block junctions are confined to the interfaces, and diffusion along the interfaces proceeds only when the PEP block retracts through the entanglements into the interfacial zone and then relaxes into a new configuration.

4.4. The cylindrical hexagonal morphology

In the hexagonal state, anisotropic diffusion along the cylinder interfaces was also observed by FRS on a hexagonal PEO-PEE sample, in addition to diffusion in imperfectly ordered regions (Hamersky *et al* 1998a). In an entangled PEP-PEE sample in the cylindrical morphology, on the other hand, no anisotropy of diffusion could be detected using FRS (Lodge *et al* 1997), and it was concluded that the activation barriers for perpendicular and parallel diffusion in this sample are similar. In a poly(styrene-*b*-methylphenylsiloxane) diblock copolymer sample, a single diffusive process was observed in PCS, and it was assigned to the translational diffusion of cylinders (Vogt *et al* 1993).

For a PEP-PDMS sample in the hexagonal state, the PFG NMR echo attenuation curves deviate substantially from the exponential shape, and a model describing anisotropic diffusion was applied (Rittig *et al* 1999) (figure 3(a)). The local mean-square displacement was split up as follows:

$$\langle z^2(t)\rangle = 2t\,(D_{\mathrm{par}}\cos^2\theta + D_{\mathrm{perp}}\sin^2\theta) \tag{9}$$

with D_{par} and D_{perp} the diffusion along the cylinder axis or perpendicular to the cylinder axis, respectively, and θ the angle between the z-axis and the cylinder under consideration. The sample was not macroscopically aligned, and consisted of cylindrical domains oriented in all directions. Therefore, equation (9) has to be averaged over all directions θ. The echo attenuation then reads

$$\Psi(q,t) = \int_0^1 \exp[-q^2 t\,(D_{\mathrm{par}}\cos^2\theta + D_{\mathrm{perp}}\sin^2\theta)]\,\mathrm{d}(\sin\theta). \tag{10}$$

This expression was fitted to the data with D_{par} and D_{perp} being the only fitting parameters. The average diffusion coefficient was determined using

$$D_{\mathrm{hex}} = \frac{D_{\mathrm{par}} + 2D_{\mathrm{perp}}}{3}. \tag{11}$$

D_{perp} is described by equation (5) with $\alpha = 0.8$ (Rittig *et al* 1999). Diffusion anisotropies, $D_{\mathrm{par}}/D_{\mathrm{perp}}$, as large as 80 were found deep in the hexagonal state.

This knowledge allows one to understand the PCS distribution functions on the same sample, which display two modes deep in the hexagonal state (apart from the cluster mode not shown here, figure 3(b)). The $(q^2\tau)^{-1}$-values of the slower mode coincide with the diffusion coefficients D_{hex} from PFG NMR (figure 3(c), Papadakis *et al* 2000b), and we conclude that this mode is due to the self-diffusion of copolymers along and across the cylinder interfaces. Its activation energy is similar to that of PEP, the block with the higher viscosity and thus the higher friction coefficient, i.e. the high friction of the cylinder material dominates the copolymer diffusion.

The fast PCS mode is not observed in the PFG NMR experiment (figure 3(c), Papadakis *et al* 2000b), i.e. it is due to displacements smaller than the length scales monitored in PFG NMR. We attribute it to overdamped undulations of the PEP cylinders which relax mainly by deformation of the PDMS brushes, similar to the ones in the lamellar state; see above. This is consistent with the finding that the activation energy is similar to that of PDMS, the matrix material. The fast mode is unlikely to be due to cylinder diffusion because the measured diffusion coefficient is even larger than the upper estimate found by using the Stokes–Einstein equation with the viscosity of the PDMS block and the cylinder diameter.

The anisotropy of the copolymer diffusion in macroscopically aligned PEP-PDMS with entangled PEP forming the matrix ($f_{\mathrm{PEP}} = 0.79$) was studied recently using FRS (Cavicchi and Lodge 2004). In a well-aligned sample, the anisotropy is large, with D_{perp} following a hindered diffusion mechanism, and D_{par} crosses over to a block retraction mechanism. Defects

were found to have a strong influence on D_{perp}, pointing to the difficulties of determining this quantity precisely.

To conclude, in cylindrical samples, a number of diffusional processes have been observed in different samples. Studies of the anisotropy of diffusion are often hampered by defects. Cylinder diffusion remains a subject to be studied. PFG NMR allowed us to quantify the anisotropy of diffusion in a non-aligned sample. Additional PCS measurements revealed an additional, faster process, which we attribute to the relative movement of cylinders.

4.5. The micellar body-centred cubic state

The micellar body-centred cubic state is qualitatively different from the morphologies discussed above because the micelles form closed entities—and not continuous structures like lamellae or cylinders—and long-range copolymer diffusion must therefore be an activated process. The diblock copolymer diffusion through the bcc structure as well as the relaxation of the copolymer end-to-end vector have been simulated using the lattice bond-fluctuation model, and it was found that the chains diffuse over a long range only if the repulsion is below a certain value; above that value, sub-diffusive behaviour is observed (Hoffmann *et al* 1997). A Langevin dynamics simulation with a spring and bead model for Rouse dynamics and the reptational Langevin dynamics have been applied to diffusion of asymmetric diblock copolymers in the body-centred cubic state, and both for Rouse chains and for reptating chains, activated diffusion was found (Yokoyama *et al* 2000).

Several experimental studies have dealt with the diblock copolymer self-diffusion in the bcc state (Yokoyama and Kramer 1998, Yokoyama *et al* 1998, Cavicchi and Lodge 2003). Using FRES, it was found that in poly(styrene-*b*-(2-vinylpyridine)) (PS-P2VP) diblock copolymer melts, the block copolymer diffusion coefficient, D, is reduced by a factor of $\sim 10^4$ compared to that of polystyrene homopolymers having the same molar mass, D_0, and the normalized diffusion coefficient D/D_0 follows approximately equation (5) with $\alpha = 1.2$ (Yokoyama and Kramer 1998, Yokoyama *et al* 1998). These findings indicate that the diffusion of PS-P2VP diblock copolymers is governed by the thermodynamic barrier for the motion of P2VP blocks from one micellar core to the other. It was further argued that the polydispersity of the P2VP block length leads to a distribution of diffusivities. Coincidence between the D/D_{hom}-values from the simulations by Yokoyama *et al* (2000) with those from FRS measurements on asymmetric PEP-PDMS samples in the bcc state (PEP being the majority component) was reported by Cavicchi and Lodge (2003), where it was concluded that the FRS decay observed is due to copolymer diffusion hindered by the bcc structure.

In the PEP-PDMS sample studied by us (23 600 g mol^{-1}, $f_{\mathrm{PEP}} = 0.16$, Papadakis *et al* 2004) forming PEP micelles in a PDMS matrix, two modes with q^2-dependent relaxation rates are observed using PCS (figures 4(b), (c)). From the Arrhenius representation (figure 4(e)), the activation energy of the fast mode is found to be similar to that of pure PDMS. The slow mode is slower than the self-diffusion of PEP homopolymers having the same molar mass as the block copolymer.

The PFG NMR echo attenuations of the same sample were not single-exponential, which may be attributed to a distribution of diffusion coefficients. A log-normal distribution of diffusion coefficients described the curves well (figure 4(d)), and it was found that the slow PCS mode in the bcc state coincides with the average self-diffusion coefficient from PFG NMR (figures 4(e), (f)), i.e. it is due to the long-range self-diffusion. The slow PCS mode is due the long-range diffusion of single copolymers from micelle to micelle. This is corroborated by the coincidence found between the dependence of the D/D_{hom}-values on χNf (f being the volume fraction of the minority component) of the PEP-PDMS sample studied by us, and

results from chemically different samples and from simulations (figure 4(g)). The fast PCS mode is not observed in the PFG NMR experiment, and we attribute it to fluctuations of the micellar distance which relax by diffusion of copolymers through the PDMS matrix.

We conclude that, in the bcc state, activated copolymer diffusion as well as the diffusion of copolymers through the matrix are at the origin of the observed modes.

5. Conclusion and perspectives

Mesoscopically structured block copolymer melts constitute a model system for studying the influence of morphology and interfaces on the slow dynamics in soft, self-organized matter. Both the copolymer self-diffusion and the collective dynamics are strongly influenced by the structures formed. The combination of several methods has proven to be very useful in order to elucidate these relations. Our review shows that the results from chemically different systems are sometimes contradictory, and systematic studies on the same sample system in different morphologies, trying to minimize the variation of other properties like the degree of entanglement, are necessary to gain a conclusive image. The studies of macroscopically aligned samples reported in the literature have advanced the field substantially; however, our careful analyses of the PFG NMR echo attenuation curves of non-aligned samples may also lead to quantitative results for diffusion mechanisms and anisotropies. The combination of PFG NMR with PCS proved to be very useful in order to determine the origin of the modes observed in PCS. The sample system chosen by us, PEP-PDMS diblock copolymers, has the advantage that a large temperature range may be studied and that the friction coefficients of the two blocks differ, which helps in assigning the processes observed. The low friction coefficient of PDMS allowed us to observe modes which in other systems may be too slow to be detected.

A new trend in the field of polymer dynamics is to probe the single-molecule dynamics in order to obtain more information about the fundamental modes of molecular motion. The direct visualization of a diffusing single molecule which recently has become possible is very exciting and seems to offer a wealth of new possibilities (Käs *et al* 1994, Humphrey *et al* 2002, Schuster *et al* 2002). So far, mainly biological macromolecules such as single actin filaments have been in the focus because they can be observed under the light microscope due to their large size. Also, non-visualizing single-molecule methods, such as fluorescence correlation spectroscopy (Elson and Magde 1974, Rigler and Elson 2000), have recently been used for diffusional studies of synthetic polymers, and they offer exciting new possibilities because of their high spatial and temporal resolution (Erhardt *et al* 2001, Bonné *et al* 2004, Zettl *et al* 2004).

Acknowledgments

This paper is dedicated to the memory of G Fleischer (†). We are grateful to F Kremer, J Kärger, F Stallmach, S Gröger, K Mortensen, K Almdal, M E Vigild, P Štěpánek, F Boué, A Lapp, J-U Sommer, C N Likos, E Straube and W Brown for support, help with the experiments, and discussions as well as critical reading of the manuscript. We gratefully acknowledge Deutsche Forschungsgemeinschaft for financial support, also within the Sonderforschungsbereich 294 'Moleküle in Wechselwirkung mit Grenzflächen' as well as the Graduiertenkolleg 'Physikalische Chemie der Grenzflächen', the Grant Agency of the Academy of Sciences of the Czech Republic, the Danish Technical Research Council through the Danish Polymer Centre and the European Commission through the Access to Research Infrastructures action of the Improving Human Potential Programme.

References

Akcasu A Z and Tombakoglu M 1990 *Macromolecules* **23** 607
Almdal K, Hillmyer M A and Bates F S 2002 *Macromolecules* **35** 7685
Almdal K, Mortensen K, Ryan A J and Bates F S 1996 *Macromolecules* **29** 5940
Almdal K, Rosedale J H, Bates F S, Wignall G D and Fredrickson G H 1990 *Phys. Rev. Lett.* **65** 1112
Anastasiadis S H 2000 *Curr. Opin. Colloid Interface Sci.* **5** 324
Anastasiadis S H, Fytas G, Vogt S and Fischer E W 1993a *Phys. Rev. Lett.* **70** 2415
Anastasiadis S H, Fytas G, Vogt S, Gerharz B and Fischer E W 1993b *Europhys. Lett.* **22** 619
Anderson D A and Wennerström H 1990 *J. Phys. Chem.* **94** 8683
Appel M and Fleischer G 1993 *Macromolecules* **26** 5520
Baltá Calleja F J and Roslaniec Z (ed) 2000 *Block Copolymers* (New York: Dekker)
Barrat J-L and Fredrickson G H 1991 *Macromolecules* **24** 6378
Bates F S 1991 *Science* **251** 898
Bates F S and Fredrickson G H 1990 *Annu. Rev. Phys. Chem.* **41** 525
Bates F S, Rosedale J H, Bair H E and Russell T P 1989 *Macromolecules* **22** 2557
Bates F S, Rosedale J H, Fredrickson G H and Glinka C J 1988 *Phys. Rev. Lett.* **61** 2229
Bonné T B, Lüdtke K, Jordan R, Štěpánek P and Papadakis C M 2004 *Colloid Polym. Sci.* **282** 833
Borsali R and Vilgis T A 1990 *J. Chem. Phys.* **93** 3610
Brandrup J and Immergut E H 1989 *Polymer Handbook* 3rd edn (New York: Wiley)
Budkowski A, Losch A and Klein J 1995 *Israel J. Chem.* **35** 55
Callaghan P T 1993 *Principles of Nuclear Magnetic Resonance* 1st edn (Oxford: Clarendon)
Cavicchi K A and Lodge T P 2003 *Macromolecules* **36** 7158
Cavicchi K A and Lodge T P 2004 *Macromolecules* **37** 6004
Chaturvedi U K, Steiner U, Zak O, Krausch G, Schatz G and Klein J 1990 *Appl. Phys. Lett.* **56** 1228
Chitanvis S M 1998 *Phys. Rev.* E **57** 1921
Colby R H 1996 *Curr. Opin. Colloid Interface Sci.* **1** 454
Dalvi M C, Eastman C E and Lodge T P 1993 *Phys. Rev. Lett.* **71** 2591
Dalvi M C and Lodge T P 1993 *Macromolecules* **26** 859
Dalvi M C and Lodge T P 1994 *Macromolecules* **27** 3487
Doyle B L and Peercy P S 1979 *Appl. Phys. Lett.* **34** 811
Ehlich D, Takenaka M and Hashimoto T 1993 *Macromolecules* **26** 492
Elson E L and Magde D 1974 *Biopolymers* **13** 1
Erhardt R, Böker A, Zettl H, Kaya H, Pyckhout-Hintzen W, Krausch G, Abetz V and Müller A H E 2001 *Macromolecules* **34** 1069
Feiweier T, Geil B, Pospiech E-M, Fujara F and Winter R 2000 *Phys. Rev.* E **62** 8182
Fetters L J, Lohse D J, Richter D, Witten T A and Zirkel A 1994 *Macromolecules* **27** 4639
Fleischer G and Fujara F 1994 *NMR—Basic Principles and Progress* **30** 159
Fleischer G, Fujara F and Stühn B 1993 *Macromolecules* **26** 2340
Fleischer G, Kärger J and Stühn B 1997 *Colloid Polym. Sci.* **275** 807
Fleischer G, Rittig F, Štěpánek P, Almdal K and Papadakis C M 1999 *Macromolecules* **32** 1956
Folkes M J and Keller A 1973 *The Physics of Glassy Polymers* ed R N Haward (London: Applied Science Publishers Ltd) p 548
Fredrickson G H and Bates F S 1996 *Annu. Rev. Mater. Sci.* **26** 501
Fredrickson G H and Helfand E 1987 *J. Chem. Phys.* **87** 697
Fredrickson G H and Milner S T 1990 *Mater. Res. Soc. Symp. Proc.* **177** 169
Fytas G and Anastasiadis S H 1994 *Disorder Effects on Relaxation Processes* ed R Richert and A Blumen (Berlin: Springer) p 697
Fytas G, Anastasiadis S H and Semenov A N 1994 *Macromol. Symp.* **79** 117
Gerharz B, Fischer E W and Fytas G 1991 *Polym. Commun.* **32** 469
Genz U and Vilgis T A 1994 *J. Chem. Phys.* **101** 7111
Guenza M and Schweizer K S 1998 *J. Chem. Phys.* **108** 1271
Guenza M, Tang H and Schweizer K S 1997 *Macromolecules* **30** 3423
Guenza M, Tang H and Schweizer K S 1998 *J. Chem. Phys.* **108** 1257
Hadziioannou G and Skoulios A 1982 *Macromolecules* **15** 258
Hajduk D A, Harper P E, Gruner S M, Honeker C C, Kim G, Thomas E L and Fetters L J 1994 *Macromolecules* **27** 4063
Hamersky M W, Hillmyer M A, Tirrell M, Bates F S, Lodge T P and von Meerwall E D 1998a *Macromolecules* **31** 5363

Hamersky M W, Tirrell M and Lodge T P 1996 *J. Polym. Sci.* B **34** 2899
Hamersky M W, Tirrell M and Lodge T P 1998b *Langmuir* **14** 6974
Hamley I W 1998 *The Physics of Block Copolymers* (Oxford: Oxford University Press)
Hamley I W, Gehlsen M D, Khandpur A K, Koppi K A, Rosedale J H, Schulz M F, Bates F S, Almdal K and Mortensen K 1994 *J. Physique* II **4** 2161
Hamley I W, Koppi K A, Rosedale J H, Bates F S, Almdal K and Mortensen K 1993 *Macromolecules* **26** 5959
Hasegawa H and Hashimoto T 1996 *Comprehensive Polymer Science. Second Supplement* ed S L Aggarwal and S Russo (London: Pergamon) p 497
Hashimoto T 1996 *Thermoplastic Elastomers* ed G Holden, N R Legge, R Quirk and H E Schroeder (Munich: Hanser) p 429
Hashimoto T, Shibayama M and Kawai H 1980 *Macromolecules* **13** 1237
Helfand E 1992 *Macromolecules* **25** 492
Hillmyer M A, Bates F S, Almdal K, Mortensen K, Ryan A J and Fairclough J P A 1996 *Science* **271** 976
Hoffmann A, Koch T and Stühn B 1993 *Macromolecules* **26** 7288
Hoffmann A, Sommer J-U and Blumen A 1997 *J. Chem. Phys.* **107** 7559
Holmqvist P, Pispas S, Hadjichristidis N, Fytas G and Sigel R 2003 *Macromolecules* **36** 830
Holmqvist P, Pispas S, Sigel R, Hadjichristidis N and Fytas G 2002 *Macromolecules* **35** 3157
Humphrey D, Duggan C, Saha D, Smith D and Käs J 2002 *Nature* **416** 413
Jakeš J 1988 *Czech. J. Phys.* B **38** 1305
Jian T, Semenov A N, Anastasiadis S H, Fytas G, Yeh F-J, Chu B, Vogt S, Wang F and Roovers J E L 1994 *J. Chem. Phys.* **100** 3286
Joabsson F, Nydén M, Linse P and Söderman O 1997 *J. Phys. Chem.* B **101** 9710
Kanetakis J and Fytas G 1991 *J. Non-Cryst. Solids* **131–133** 823
Kanetakis J, Fytas G, Kremer F and Pakula T 1992 *Macromolecules* **25** 3484
Kärger J, Fleischer G and Roland U 1998 *Diffusion in Condensed Matter* ed J Kärger *et al* (Braunschweig: Vieweg) p 144
Kärger J, Papadakis C M and Stallmach F 2004 *Molecules in Interaction with Surfaces* (*Springer Lecture Notes in Physics*) ed R Haberlandt, D Michel, A Pöppl and R Stannarius (Heidelberg: Springer) p 125
Kärger J, Pfeifer H and Heink W 1988 *Adv. Magn. Res.* **12** 1
Kärger J, Stallmach F and Vasenkov S 2003 *Magn. Reson. Imag.* **21** 185
Käs J, Strey H and Sackmann E 1994 *Nature* **368** 226
Kerle T, Scheffold F, Losch A, Steiner U, Schatz G and Klein J 1997 *Acta Polym.* **48** 548
Laradji M, Shi A-C, Desai R C and Noolandi J 1997 *Phys. Rev. Lett.* **78** 2577
Lodge T 1994 *Mikrochim. Acta* **116** 1
Lodge T and Chapman B 1997 *Trends Polym. Sci.* **5** 128
Lodge T P and Dalvi M C 1995 *Phys. Rev. Lett.* **75** 657
Lodge T P, Hamersky M W, Milhaupt J M, Kannan R M, Dalvi M C and Eastman C E 1997 *Macromol. Symp.* **121** 219
Matsushita Y, Mori K, Saguchi R, Nakao Y, Noda I and Nagasawa M 1990 *Macromolecules* **23** 4313
Mills P J, Green P F, Palmstrøm C J, Mayer J W and Kramer E J 1984 *Appl. Phys. Lett.* **45** 957
Mortensen K 2000 *Scattering in Polymeric and Colloidal Systems* ed W Brown and K Mortensen (Amsterdam: Gordon and Breach) p 413
Murat M, Grest G C and Kremer K 1998 *Europhys. Lett.* **42** 401
Nydén M and Söderman O 1995 *Langmuir* **11** 1537
Papadakis C M, Almdal K, Mortensen K and Posselt D 1996 *Europhys. Lett.* **36** 289
Papadakis C M, Almdal K, Mortensen K and Posselt D 1997 *J. Physique* II **7** 1829
Papadakis C M, Almdal K, Mortensen K, Rittig F, Fleischer G and Štěpánek P 2000a *Eur. Phys. J.* E **1** 275
Papadakis C M, Almdal K, Mortensen K, Rittig F and Štěpánek P 2000b *Macromol. Symp.* **162** 275
Papadakis C M, Almdal K, Mortensen K, Vigild M E and Štěpánek P 1999 *J. Chem. Phys.* **111** 4319
Papadakis C M, Brown W, Johnsen R M, Posselt D and Almdal K 1996 *J. Chem. Phys.* **104** 1611
Papadakis C M, Rittig F, Almdal K, Mortensen K and Štěpánek P 2004 *Eur. Phys. J.* E **15** 359
Pearson D S, Fetters L J, Graessley W W, Ver Strate G and von Meerwall E 1994 *Macromolecules* **27** 711
Provencher S W 1982 *Comput. Phys. Commun.* **27** 229
Qi S and Wang Z-G 1996 *Phys. Rev. Lett.* **76** 1679
Ribotta R, Salin D and Durand G 1974 *Phys. Rev. Lett.* **32** 6
Richards R W and Thomason J L 1983 *Macromolecules* **16** 982
Rigler R and Elson E (ed) 2000 *Fluorescence Correlation Spectroscopy. Theory and Applications* (Berlin: Springer)
Rittig F, Fleischer G, Kärger J, Papadakis C M, Almdal K and Štěpánek P 1999 *Macromolecules* **32** 5872

Rittig F, Kärger J, Papadakis C M, Fleischer G, Almdal K and Štěpánek P 2001 *Macromolecules* **34** 868
Ryan A J and Hamley I W 1997 *The Physics of Glassy Polymers* ed R N Haward and R J Young (London: Chapman and Hall) p 451
Schulz M F, Bates F S, Almdal K and Mortensen K 1994 *Phys. Rev. Lett.* **73** 86
Schuster J, Cichos F and von Borczyskowski C 2002 *J. Phys. Chem.* A **106** 5403
Semenov A N, Fytas G and Anastasiadis S H 1994 *Polymer Preprints (Am. Chem. Soc., Div. Polym. Chem.)* **35** 618
Shull K R, Kramer E J, Bates F S and Rosedale J H 1991 *Macromolecules* **24** 1383
Sigel R, Pispas S, Hadjichristidis N, Vlassopoulos D and Fytas G 1999 *Macromolecules* **32** 8447
Štěpánek P 1993 *Dynamic Light Scattering. The Method and Some Applications* ed W Brown (Oxford: Clarendon) p 177
Štěpánek P, Almdal K and Lodge T P 1997 *J. Polym. Sci., Polym. Phys. Edn* **35** 1643
Štěpánek P and Johnsen R M 1995 *Collect. Czech. Chem. Commun.* **60** 1941
Štěpánek P and Lodge T P 1996a *Light Scattering. Principles and Development* ed W Brown (Oxford: Clarendon) p 343
Štěpánek P and Lodge T P 1996b *Macromolecules* **29** 1244
Štěpánek P and Lodge T P 1997 *Light Scattering and Photon Correlation Spectroscopy* ed E R Pike and J B Abbiss (Dordrecht: Kluwer–Academic) p 189
Štěpánek P, Nallet F and Almdal K 2001 *Macromolecules* **34** 1090
Tang H and Schweizer K S 1995 *J. Chem. Phys.* **103** 6296
Vigild M E 1997 *PhD Thesis* University of Copenhagen, Denmark
Vigild M E, Almdal K, Mortensen K, Hamley I W, Fairclough J P A and Ryan A J 1998 *Macromolecules* **31** 5702
Vogt S, Anastasiadis S H, Fytas G and Fischer E W 1994 *Macromolecules* **27** 4335
Vogt S, Gerharz B, Fischer E W and Fytas G 1992 *Macromolecules* **25** 5986
Vogt S, Jian T, Anastasiadis S H, Fytas G and Fischer E W 1993 *Macromolecules* **26** 3357
Yokoyama H and Kramer E J 1998 *Macromolecules* **31** 7871
Yokoyama H and Kramer E J 2000a *Macromolecules* **33** 954
Yokoyama H and Kramer E J 2000b *Macromolecules* **33** 1871
Yokoyama H, Kramer E J and Fredrickson G H 2000 *Macromolecules* **33** 2249
Yokoyama H, Kramer E J, Rafailovich M H, Sokolov J and Schwarz S A 1998 *Macromolecules* **31** 8826
Zettl H, Häfner W, Böker A, Schmalz H, Lanzendörfer M, Müller A H E and Krausch G 2004 *Macromolecules* **37** 1917
Zielinski J M, Heuberger G, Sillescu H, Wiesner U, Heuer A, Zhang Y and Spiess H W 1995 *Macromolecules* **28** 8287